Front. Chem. Sci. Eng. 2021, 15(2): 421–436
https://doi.org/10.1007/s11705-020-1952-7

RESEARCH ARTICLE

Biodegradation and detoxification of the triphenylmethane dye coomassie brilliant blue by the extracellular enzymes from mycelia of *Lactarius deliciosus*

Jin Zhao[1], Qing-Xi Wu (✉)[1,2], Xiao-Du Cheng[1], Ting Su[1], Xiao-Hui Wang[1], Wen-Na Zhang[1,2], Yong-Ming Lu[1,2], Yan Chen (✉)[1,2]

1 School of Life Sciences, Anhui University, Hefei 230601, China
2 Anhui Key Laboratory of Modern Biomanufacturing, Hefei 230601, China

Abstract Fungi play an important role in dying wastewater treatment. In this work, the mycelia of *Lactarius deliciosus* exhibited an excellent capacity in decolorizing coomassie brilliant blue (CBB). The results demonstrated that the mycelia could treat CBB with high concentrations over a broad range of pH and temperature. The decolorization rate of 99.19% and the removal rate of 16.31 $mg \cdot L^{-1} \cdot h$ were realized. The mycelia could be recycled from decolorizing process for 19 times, indicating a good re-usability. It verified that the lignin peroxidase (121.65 $U \cdot L^{-1}$) and manganese peroxidase (36.77 $U \cdot L^{-1}$) were involved in the degradation and decolorization process of CBB. Toxicity assessments indicated the seed germination rate was up to 82.22% while inhibition to *Escherichia coli* decreased dramatically and no significant effect on *Caenorhabditis elegans* growth was found. The removal of CBB was a synergistic process accomplished by adsorption and biodegradation. The mycelia could be used for eco-friendly CBB treatment.

Keywords fungus mycelia, biodegradation, extracellular enzymes, coomassie brilliant blue, *Lactarius deliciosus*

1 Introduction

In recent years, with the booming industries of textile, printing and dying, more than 100000 kinds of commercial dyes have been explored for relevant purposes. However, about 10%–15% of the dyes are discharged without proper treatment during production and usage [1], which has caused huge pollution to the environment and has brought significant health risks [2–4]. More than 700000 tonnes of dye wastewater is produced each year, which contains a variety of dyes (10–200 $mg \cdot L^{-1}$) and some other organic/inorganic chemicals [5]. Textile dyes in wastewater have certain toxic effects on some plants' germination while influencing their total biomass [6]. Therefore, it's urgent to seek solutions for treating the dye wastewater.

According to their chemical structures, synthetic dyes can be classified into azo dyes, triphenylmethane dyes, anthraquinone dyes, heterocyclic dyes, indigo dyes and aromatic methane dyes [7]. Among them, azo, anthraquinone and triphenylmethane dyes rank the top three in terms of industrial production [8–10]. Triphenylmethane dyes are a type of aromatic chemical colorants, in which the central carbon atom is linked to three phenyl groups [11]. They have caused increasing environmental concerns due to their potential toxicity to animals and humans [12]. For example, direct contact of malachite green would irritate skin painfully and exert permanent injury on human and animal eyes [13]. Also, crystal violet dyes have been confirmed to be toxic to mammalian cells, and could be mutagen and mitotic poison to organisms [14]. Considering the wide use of dyes in textile, pharmaceutical, cosmetic, leather and food industries, dying wastewater has thus become one of the most common industrial pollutant headstreams [15,16]. It contains both harmful substances which hardly degrade in natural environment and some dyes that may break down into secondary pollutants undesirably [17]. Thus, there's an urgent need to address the issue.

At present, technologies used for dying wastewater treatment fall into three categories: physical, chemical and biological [18–22]. Traditional treatment includes coagu-

Received January 12, 2020; accepted April 22, 2020

E-mails: wuqx@ahu.edu.cn (Wu Q-X), chenyan@ahu.edu.cn (Chen Y)

lation, flocculation with lime, ozonation, oxidation, electrolysis, adsorption on activated charcoal [23–26]. Overall, the physicochemical methods have several limitations: (1) The economical infeasibility, i.e., they are costly due to the consumption of much more energy and chemical reagents [6]; (2) the inability to completely remove some stubborn dyes or their organic metabolites [4]; (3) the production of a large amount of sewage sludge which can cause secondary pollution [27]; (4) the demand for tertiary treatment like photochemical, ozonation processes [28]; (5) the lack of efficiency in solving the toxicity problem thoroughly [29]. Thus, considering the strength of being environment-friendly, biological treatments like microbial decolorization and degradation are being studied by researchers [16,30,31]. In this treatment process, microorganisms can adapt to the growing environment containing waste dyes and convert them into harmless metabolites by using certain types of enzymes, such as ligninolytic enzymes, namely laccase, manganese peroxidase (MnP) and lignin peroxidase (LiP) [15,32].

By far, different kinds of bacteria, fungi and yeast species have been found to be able to decolorize dyes through bioadsorption and/or degradation [12]. Besides, it has been confirmed that the white rot fungi are capable of decolorizing textile dyes or colored effluents, such as *Trametes versicolor*, *Trametes hispida* [33]. Coomassie brilliant blue G-250 (CBB) is a triphenylmethane dye originally used in the textile industry [34]. It's also commonly used for the analysis of staining proteins in biochemical, pharmaceutical and medical researches [35].

In this work, a type of fungus *Lactarius deliciosus* developed for decolorization of triphenylmethane dye was discovered. The objectives of this study were to investigate the potential of the obtained mycelia on decolorizing CBB and to optimize parameters including dye concentration, temperature, pH, agitation speed for a purpose of improving CBB degrading efficiency and illuminating the effects of main enzymes functioning during the degradation process. The enzymatic activities of the enzymes with varied pH at different temperatures were investigated, and the kinetic parameters of the enzymes were determined under optimal conditions. In addition, fourier transform infrared spectroscopy (FTIR) and scanning electron microscopy (SEM) analysis were used to characterize the metabolites and observe the fungi morphology variation. The fluorescent inverted microscope, ultra-violet-visible (UV-vis) spectrophotometer and thermal gravimetric analysis (TG/DTG) were used to evaluate the dye decolorization properties. Meanwhile, the toxicity of residual CBB dyes in solutions was evaluated by phytotoxicity, microbial and *Caenorhabditis elegans* assays. For a potential practical application, the successive batched decolorization experiments of the mycelia were also investigated.

2 Experimental

2.1 Materials

The edible fungi fruiting bodies of the wild *L. deliciosus* were sampled and purchased from Qianshan county, Anqing city, Anhui province. The mycelia were activated and cultivated from the fruiting bodies and purified with plates for several times. Then the liquid fermentation of the mycelia took place in the shakers for the subsequent experiments. The mycelia were maintained on plates with the potato dextrose agar media at 4 °C and were subcultured every two weeks.

Caenorhabditis elegans (N2, wild type) were presented by Professor Aifang Du from Zhejiang University. CBB (C.I.42655) used in this study was purchased from Sigma, Shanghai, China. 2,2-Azinobis (3-ethylbenzothiazolin-6-sulfonic acid) (ABTS) and 3,4-dimethoxybenzyl alcohols were obtained from Macklin Biochemical Technology Company (Shanghai, China).

2.2 Cultivation of the mycelia

The mycelia pellets of *L. deliciosus* cultivated for CBB removal experiments were carried out in erlenmeyer flasks (250 mL) with the liquid culture media (LCM), which contained 2.8% glucose (w/v), 0.4% KH_2PO_4 (w/v), 0.2% anhydrous $MgSO_4$ (w/v), 0.4% yeast extract (w/v).

2.3 CBB decolorization experiments

The CBB dye removal experiments were conducted in 250 mL erlenmeyer flasks at 28 °C, 120 $r \cdot min^{-1}$. The CBB dye was dissolved in LCM (pH 5.0) at different concentrations (25–800 $mg \cdot L^{-1}$), then autoclaved at 121 °C for 20 min. The samples were collected at intervals of 12 h and centrifuged at 6000 $r \cdot min^{-1}$ for 5 min. The CBB contents in the supernatant were measured using a double beam spectrophotometer (UV 1901, PERSEE, Beijing, China) at 588 nm [3]. The percentage of CBB decolorization rates were calculated using the following formula [27,36]:

$$Decolorization\ \ (\%) = (C_0 - C_t)/C_0 \times 100. \quad (1)$$

The CBB removal rates ($mg \cdot L^{-1} \cdot h$) were calculated using the following formula [32]:

$$Rate\ of\ removal = (C_0 - C_t)/t, \quad (2)$$

where C_0 and C_t represent dye concentrations ($mg \cdot L^{-1}$) before and after a certain process time t, respectively.

2.4 Effects of different parameters on CBB decolorization

2.4.1 Effects of static and shaking conditions

The effects of static and shaking conditions on the

decolorization of CBB dye were investigated in erlenmeyer flasks containing 120 mL of LCM with sterilized CBB dye of 50 $mg \cdot L^{-1}$. The mycelia were incubated respectively into the sterilized LCM containing CBB and cultured under shaking conditions (0, 90, 120, 150, 180 $r \cdot min^{-1}$) at 28 °C.

2.4.2 Effects of physicochemical parameters

The effects of different physicochemical parameters of temperature and pH on the decolorization of CBB dye were also studied in erlenmeyer flasks as indicated in Section 2.4.1. The mycelia were inoculated into the sterilized LCM and cultured under shaking conditions (120 $r \cdot min^{-1}$) at different pH values (3, 5, 7, 9, 11) and temperatures (16 °C, 22 °C, 28 °C, 34 °C) correspondingly.

2.4.3 Effects of initial CBB dye concentrations

In order to study the effects of increasing dye concentrations on decolorization capacity of the mycelia, the experiments were carried out with CBB dyes of 25–800 $mg \cdot L^{-1}$. All the tests were performed in 250 mL erlenmeyer flasks under conditions at pH 5.0, 28 °C, 120 $r \cdot min^{-1}$.

2.5 Decolorization with successive batches

The mycelia were inoculated into the sterilized LCM containing 50 $mg \cdot L^{-1}$ CBB dye at 28 °C, pH 5.0, 120 $r \cdot min^{-1}$. The samples were taken at intervals of 12 h and centrifuged at 6000 $r \cdot min^{-1}$ for 5 min, then collected and measured with spectrophotometer at 588 nm. After the decolorization process, mycelia pellets were filtered and rinsed with distilled water before being transferred into fresh LCM (50 $mg \cdot L^{-1}$ CBB) for the next treatment batch.

2.6 Extracellular enzyme activities and kinetics assays

The activity of laccase was determined by ABTS oxidation method [18]. The reaction system contained 2 mL sodium acetate buffer (0.2 $mol \cdot L^{-1}$, pH 4.8), 0.5 $mmol \cdot L^{-1}$ ABTS and 0.5 mL enzyme. The oxidation of ABTS was measured at 420 nm (ε_{420} = 36000 $L \cdot mol^{-1} \cdot cm^{-1}$). The LiP activity was monitored at 310 nm (ε_{310} = 9300 $L \cdot mol^{-1} \cdot cm^{-1}$) in a 3 mL of reaction mixture containing 0.2 $mol \cdot L^{-1}$ sodium tartrate buffer (pH 3.0), 15 $mmol \cdot L^{-1}$ veratryl alcohol, 20 $mmol \cdot L^{-1}$ H_2O_2 and 0.4 mL enzyme [27]. For assessment of MnP activity, the standard reaction mixture (3 mL) containing 0.2 $mol \cdot L^{-1}$ sodium acetate buffer (pH 4.8), 1.6 $mmol \cdot L^{-1}$ $MnSO_4$, 1.6 $mmol \cdot L^{-1}$ H_2O_2 and 0.4 mL enzyme solution was used. The oxidation of substrate was assessed at 240 nm (ε_{240} = 6500 $L \cdot mol^{-1} \cdot cm^{-1}$) [37]. One unit of enzyme activity was defined as 1 $\mu mol \cdot L^{-1}$ of substrate oxidized per minute or 1 $\mu mol \cdot L^{-1}$ product generated per minute under the preconditions [38]. Meanwhile, the variation of biomass and pH was examined during the decolorization process.

Furthermore, the maximum activities of the above extracellular enzymes at different temperatures (30 °C–70 °C) and pH (2.0–10.0) values were evaluated. At the optimum temperature and pH conditions, different concentrations of ABTS (0.3, 0.4, 0.5, 0.6, 0.7 $mmol \cdot L^{-1}$), $MnSO_4$ (1.4, 1.5, 1.6, 1.7, 1.8 $mmol \cdot L^{-1}$) and veratryl alcohol (13, 14, 15, 16, 17 $mmol \cdot L^{-1}$) were prepared, and the enzyme activities were determined accordingly. The kinetic constants of the targeted enzymes were calculated subsequently.

2.7 Analytical procedures

2.7.1 Morphological characteristics analysis

The SEM (S-4800, Hitachi, Japan) and inverted fluorescence microscope (IFM, Olympas IX73, Olympas Optical Co., Ltd., Japan) were used to examine the morphological characteristics of the mycelia. The mycelia before and after treatment were further characterized by X-ray diffraction (XRD, SmartLab 9KW, Japan) analysis at 40 kV and 100 mA from 80º to 10º at the rate of $20º \cdot min^{-1}$ [39].

2.7.2 CBB conversion analysis

The biodegradation process was analyzed via the adsorption peaks variation [34]. Before the treatment, 5 mL of CBB was prepared as the standard. After decolorization process, the obtained supernatants and CBB standard were scanned through full wavelength at 190–900 nm using spectrophotometer.

The conversion products in supernatant were extracted with equal volume of ethyl acetate to obtain the fractions [32]. The extracts were kept in anhydrous Na_2SO_4 to remove water and were used for infrared spectra analysis (Fourier Transform Infrared Spectroscopy, FTIR, Nicolet 6700, Thermo Electron Co., MA, USA). The control and extracted metabolites were mixed with pure KBr powder and analyzed within the range of 400–4000 cm^{-1} [40].

2.7.3 Stability analysis

Thermal gravimetric (TG 5500, Perkin-Elmer Pyris-1, USA) analysis was conducted to check the thermometric stability of the mycelia before and after the treatment. The freeze-dried mycelia were analyzed for the weight changes (50 °C–350 °C) at a heating rate of 10 $°C \cdot min^{-1}$ in nitrogen atmosphere (10 $mL \cdot min^{-1}$) [41].

2.8 Toxicity evaluation of the decolorized water

2.8.1 Phytotoxicity assay

The phytotoxicity of the decolorized water on wheat seeds germination was evaluated. The wheat seeds were soaked in sterile distilled water overnight. Subsequently, the seeds were soaked within 1 mL of CBB dye solution (50 mg·L^{-1}) and 1 mL of the decolorized water for 3–4 times per day at room temperature, each time 1 mL of the fresh dye solution or decolorized water being used, respectively, to keep the wheat seeds in a moist environment. Meanwhile, distilled water was used in the control group. The percentage of germination, roots and plumule length were recorded at predetermined time intervals accordingly [42].

2.8.2 Contact inhibition toxicity test of *Escherichia coli*

Microbial contact toxicity was determined by spread-plate-count method [43]. The LB medium was prepared with CBB dye solution (50 mg·L^{-1}) and the decolorized water respectively, then the *E. coli* culture was spread on the plates. Distilled water was used as the control. After 12 h of incubation at 37 °C, the contact inhibition toxicity of *E. coli* was assessed by the number of colonies growing on the plates. All experiments were performed in triplicate. The inhibition rate (%) was calculated according to the following equation:

$$\text{Inhibition rate}(\%) = (A_0 - A_t)/A_0 \times 100\%. \quad (3)$$

where A_0 is the amount of *E. coli* colonies produced after being treated with distilled water, while A_t is the amount of *E. coli* colonies produced at a certain time t after being treated with the CBB dye solution or decolorized water.

2.8.3 Evaluation of toxicity on *Caenorhabditis elegans*

The toxic and behavioral influences on *C. elegans* were examined with the decolorized water under 20 °C conditions. The body length of *C. elegans* was measured under microscope, in which the experimental *C. elegans* was anesthetized with 20 mmol·L^{-1} NaN_3. Meanwhile, the movement behavior was evaluated by body bends and head thrashes during the growth. The frequency of head thrashes from one side to the other within 30 s was recorded. The frequency of body bends within 20 s was also investigated. One body bend refers to the movement of *C. elegans* in one wavelength relative to the long axis of the body. The lipofuscin accumulation was also observed via the IFM. The average fluorescence intensity of images was obtained by Image J software. At least 25 *C. elegans* were experimented in each group.

2.9 Statistical analysis

The OriginLab software (OriginPro 8.5, OriginLab Co., USA) was used to make data analysis. Experiments were conducted at least in triplicate and the results were expressed as mean ± SD.

3 Results and discussion

3.1 Mycelia cultivation and dye removal effects

As a rare and delicious wild edible fungus, *L. deliciosus* has rich nutritional values; however, it cannot be planted at present. In this experiment, the mycelia of *L. deliciosus* were successfully cultivated from the fruiting body, and then fermented in the liquid cultrue (Fig. 1), which is meaningful to the protection of their germplasm resources. Moreover, for the first time it was found that the mycelia had a good dye removal effect on CBB (triphenylmethane dye), which is an important function among the fungal mycelia. Similar researches have been done on utilizing other types of fungal mycelia pellets in removing dyes. For instance, Wang et al. reported the marine-derived *Penicillium janthinellum* mycelial pellets which were used as a kind of biosorbent [44].

3.2 Optimization of the treatment parameters for CBB decolorization efficiency

3.2.1 Effects of dye concentrations on CBB decolorization

The decolorization efficiency of the fermented mycelia of *L. deliciosus* was studied with different initial dye concentrations. It was found that the optimal dye treatment concentrations of CBB ranged from 25 to 600 mg·L^{-1} (Fig. 2(a) and Fig. 2(b)), and the maximum decolorization rates could reach more than 97% with an increasing concentration of dyes. However, the CBB decolorization

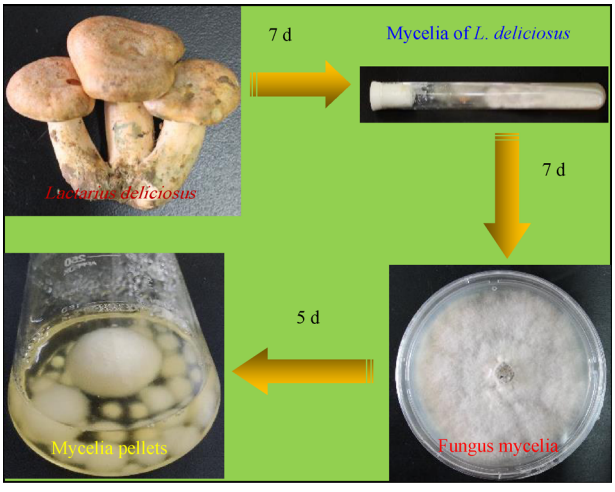

Fig. 1 Schematic illustration of the mycelia cultivation from the fruiting body of *L. deliciosus*.

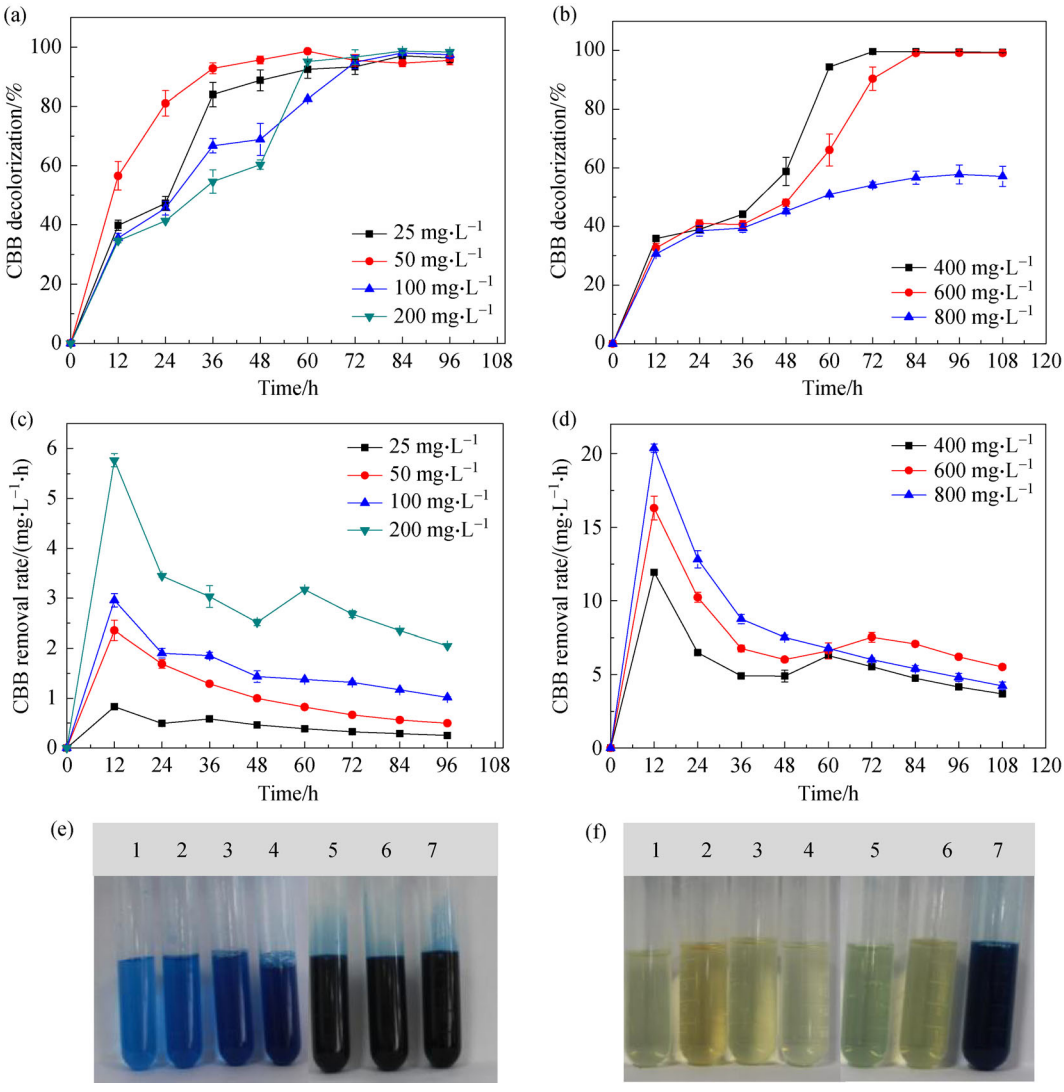

Fig. 2 Decolorization efficiency of CBB with the *L. deliciosus* mycelia performed in the culture media. (a) Decolorization rates of CBB with concentrations of 25–100 mg·L^{-1}; (b) decolorization rates of CBB with concentrations of 400–800 mg·L^{-1}; (c) removal rates of CBB with concentrations of 25–100 mg·L^{-1}; (d) removal rates of CBB with concentrations of 400–800 mg·L^{-1}; (e) CBB solutions before decolorization process with concentrations of 25, 50, 100, 200, 400, 600, 800 mg·L^{-1} presented in lanes 1–7 respectively; (f) CBB solutions after decolorization process with concentrations of 25, 50, 100, 200, 400, 600, 800 mg·L^{-1} presented in lanes 1–7 respectively.

rate was dramatically reduced to only 57.73% at the concentration of 800 mg·L^{-1} (Fig. 2(b)), indicating this concentration went beyond the dye treatment capacity of the *L. deliciosus* mycelia. Moreover, the CBB decolorization rate could go up to 99.19% in the 600 mg·L^{-1} LCM samples, while the maximal CBB removal rate was 16.31 mg·L^{-1}·h (Fig. 2(d)). Comparatively, the decolorization efficiency was lower in the 800 mg·L^{-1} LCM samples as mentioned above, which is consistent to what is reported by Chakraborty et al. [2].

Besides, as can be seen from Fig. 2(a), the CBB decolorization rate was 98.57% at 60 h after being treated with initial dye concentration of 50 mg·L^{-1}. In comparison, a longer treatment time was required for complete decolorization with increasing initial dye concentration. For instance, 96 h of treatment time was essential to achieve a decolorization rate of 99.50%, 99.19% and 57.73% for initial dye concentrations' of 400, 600 and 800 mg·L^{-1} (Fig. 2(b)), respectively. However, the 25 mg·L^{-1} LCM samples (Fig. 2(a)) exhibit a different trend, which may be ascribed to a lower dye content that slowed down CBB molecules' adsorption into the mycelia pellets, thus reducing the CBB dye's decolorization and conversion. But it was consistent with the CBB removal rate analyzed

in Fig. 2(c), where the CBB removal rate was the lowest (Max. 0.83 $mg \cdot L^{-1} \cdot h$) compared with all other samples. That is to say, as dye concentrations increase, decolorization rates display an overall downward trend. This phenomenon is also found in the *Mucoromycotina* sp. and other white rot fungi researches [7]. The results also showed that the time required for complete decolorization of initial dye concentrations of 200, 400, 600 and 800 $mg \cdot L^{-1}$ was 84, 84, 96 and 96 h respectively (Fig. 2 (a) and Fig. 2(b)).

Moreover, from the Fig. 2(e) and 2(f) we can clearly see that the CBB was well removed from the LCM with dye concentrations of 25–600 $mg \cdot L^{-1}$ in light of the color. It indicated that the mycelia of *L. deliciosus* had a good performance in treating CBB dye. More importantly, this treatment was controlled within a shorter time compared with other organisms, e.g., the complete decolorization of the reactive black (60 $mg \cdot L^{-1}$) by *T. versicolor*, *P. chrysosporium* and *Bjerkandera* sp. BOS55 was realized after 3, 2 and 4 d respectively [45]. Besides, a certain degree of color was presented in the final LCM, indicating pre-adsorption existed during the decolorization process. As is reported, the bioadsorption of dyes was probably due to the heteropolysaccharides and lipids with charged functional groups [46]. In all, the dye concentration in the biological treatment system tends to be saturated to most of the microorganisms. It thus confirmed that the increase of initial dye concentration had a far-reaching effect on the decolorization efficiency [47].

3.2.2 Effects of agitation speeds on CBB decolorization efficiency

The effects of agitation speeds on dye decolorization efficiency through the *L. deliciosus* mycelia were evaluated with 50 $mg \cdot L^{-1}$ CBB LCM samples under the static and shaking (90–180 $r \cdot min^{-1}$) conditions at 28 °C. The results showed the agitation speed of 120 $r \cdot min^{-1}$ favored the removal of CBB dye, realizing a decolorization rate of 98.57% within 60 h treatment period. While at agitation speeds of 90, 150 and 180 $r \cdot min^{-1}$, within 60 h the mycelia pellets were able to reach decolorization rates of 96.70%, 96.94% and 92.76%, respectively (Fig. 3(a)).

However, under static conditions, only 48.82% decolorization rate was achieved within the same treatment period, indicating the shaking had a positive effect on the decolorization of CBB dye. Similarly, it is reported that only 45% decolorization rate was realized under static condition in the crystal violet dye treatment system [27]. Figure 3(b) showed the CBB removal rate reached the maximal value of 2.79 $mg \cdot L^{-1} \cdot h$ at 150 $r \cdot min^{-1}$, and 2.35 $mg \cdot L^{-1} \cdot h$ at 120 $r \cdot min^{-1}$ with the minimal value of 2.02 $mg \cdot L^{-1} \cdot h$ at 90 $r \cdot min^{-1}$. The removal rates between the agitation speeds of 120 $r \cdot min^{-1}$ and 150 $r \cdot min^{-1}$ exhibited few differences. Considering energy consumption during the process, 120 $r \cdot min^{-1}$ was chosen as the optimum agitation speed for the following decolorization experiments. Agitation can directly affect the dissolved oxygen which microorganisms demand for growth, resulting in an increased rate of enzyme synthesis [5].

3.2.3 Effects of pH values on CBB decolorization efficiency

In the present study, the CBB decolorization via the *L. deliciosus* mycelia was investigated at different pH values (3–11) of the LCM at 28 °C, while the initial dye concentration (50 $mg \cdot L^{-1}$) and agitation speed of 120 $r \cdot min^{-1}$ remained unchanged. As presented in Fig. 3 (c), decolorization rates were obviously affected by pH conditions. At pH 5, a maximum dye decolorization rate of 98.57% was realized after 60 h, and decolorization rates decreased to 79.74% at pH 7, 65.06% at pH 9 and 68.21% at pH 11. It indicated that neutral and alkaline environments were unfavorable for CBB decolorization by the mycelia. However, under the strong acidic condition at pH 3, the CBB decolorization rate (67.35%) also decreased evidently. Therefore, the pH value around 5 was the optimum condition for the mycelia treatment. Meanwhile, from the Fig. 3(d) we can see that CBB removal rate was also relatively high (2.36 $mg \cdot L^{-1} \cdot h$) at pH 5 and slightly higher at pH 9 (2.43 $mg \cdot L^{-1} \cdot h$), followed by CBB removal rate at pH 3 (2.00 $mg \cdot L^{-1} \cdot h$), pH 7 (1.73 $mg \cdot L^{-1} \cdot h$) and pH 11 (2.20 $mg \cdot L^{-1} \cdot h$) respectively. Similar pH dependent decolorization results are also found in the immobilized white-rot fungi treatment system for removing the metal textile dye Lanaset Grey G. It indicated the optimum pH values for the Lanaset Grey G decolorization probably ranged between 4–6 [45]. Besides, it proved that through the controlling of the $[H^+]$ concentration, the degradation of the pollutants could be efficiently influenced [2].

3.2.4 Effects of temperatures on CBB decolorization efficiency

The effect of temperature on CBB decolorization by the *L. deliciosus* mycelia was studied in the range of 16 °C–34 °C with 50 $mg \cdot L^{-1}$ LCM samples at 120 $r \cdot min^{-1}$, pH 5. The results showed the decolorization rates were higher at 16 °C–28 °C. Figure 3(e) shows the increase of temperature could lead to the initial increase and the subsequent decrease of decolorization rates. As seen in Fig. 3(e), under the condition of 28 °C a maximum decolorization rate of 98.57% was realized after 60 h treatment; the maximal decolorization rates after 96 h were 96.83%, 96.15% and 59.96% at 16 °C, 22 °C, 34 °C respectively. Meanwhile, Fig. 3(f) shows the CBB rate has

reached the maximal value of 2.36 mg·L^{-1}·h at 28 °C, followed the CBB removal rates of 1.13 mg·L^{-1}·h at 16 °C, 1.47 mg·L^{-1}·h at 22 °C and 1.59 mg·L^{-1}·h at 34 °C. The decrease of decolorization efficiency at a higher temperature may be ascribed to the loss of cell viability [48]. Herein, 28 °C was chosen as the optimum temperature for the treatment process.

3.3 Successive batch decolorization

As can be seen from Fig. 4, the mycelia pellets could continuously treat the LCM containing CBB dye (50 mg·L^{-1}) for 19 times, and the final decolorization rate could go up to 85.50%. This outstanding recycle property has been barely mentioned in pertinent literatures. For examples, the alginate-immobilized *Trametes versicolor* could be continuously reused for six times [33]; the immobilized mixed flora of white-rot fungi (*Coriolopsis gallica*, *Bjerkandera adust*, *Trametes versicolor* and *Trametes trogii*) could be recycled for three times continuously with a 70% decolorization rate [45]. By contrast, the successive batch decolorization property was better in this study. As shown in Fig. 4(a), the first complete decolorization process was relatively long, since

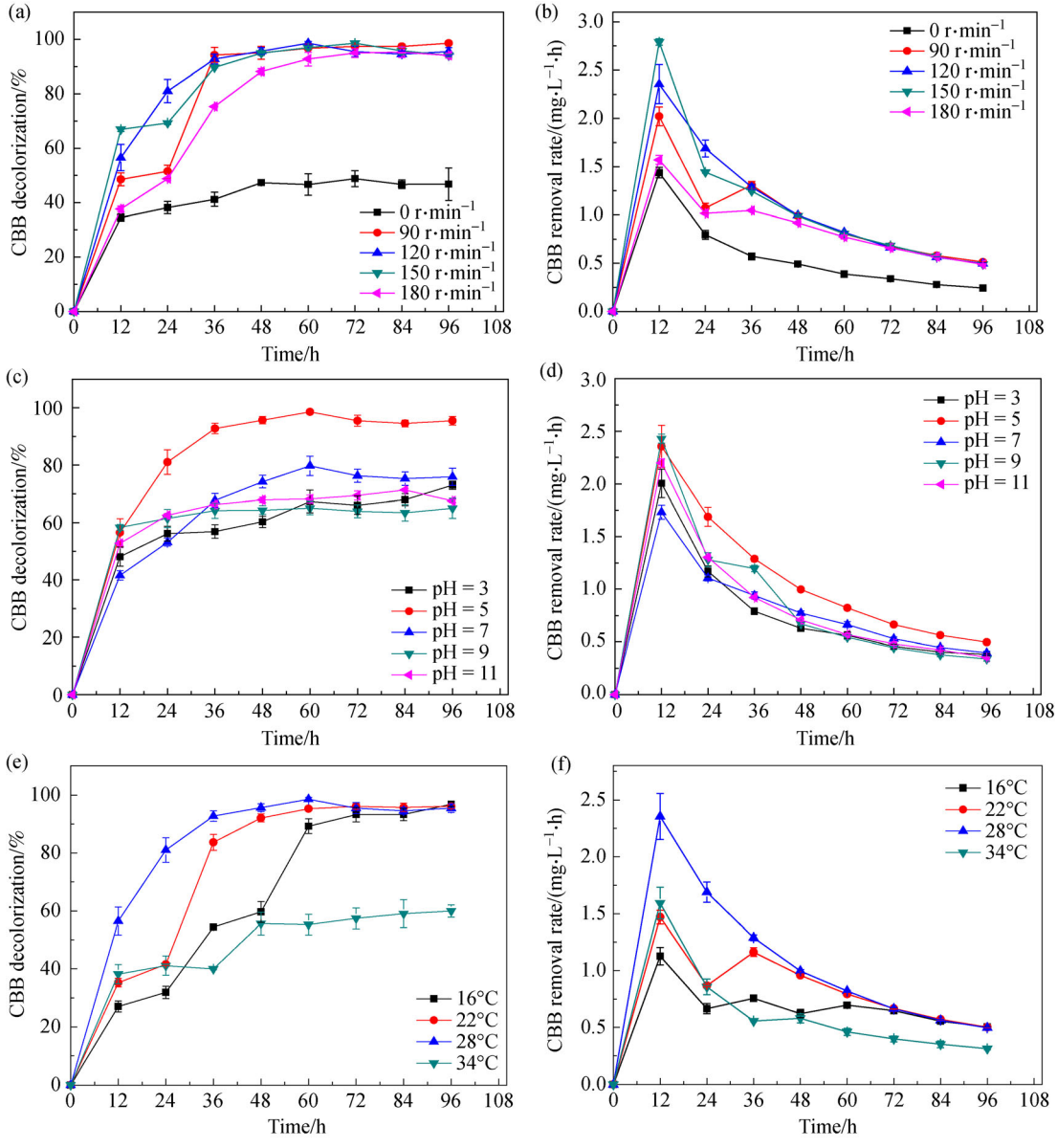

Fig. 3 Effects of treatment parameters on CBB decolorization efficiency with the 50 mg·L^{-1} samples. (a) Effect of agitation speed on CBB decolorization rates; (b) effect of agitation speed on CBB removal rates; (c) effect of pH on CBB decolorization rates; (d) effect of pH on CBB removal rates; (e) effect of temperature on CBB decolorization rates; (f) effect of temperature on CBB removal rates.

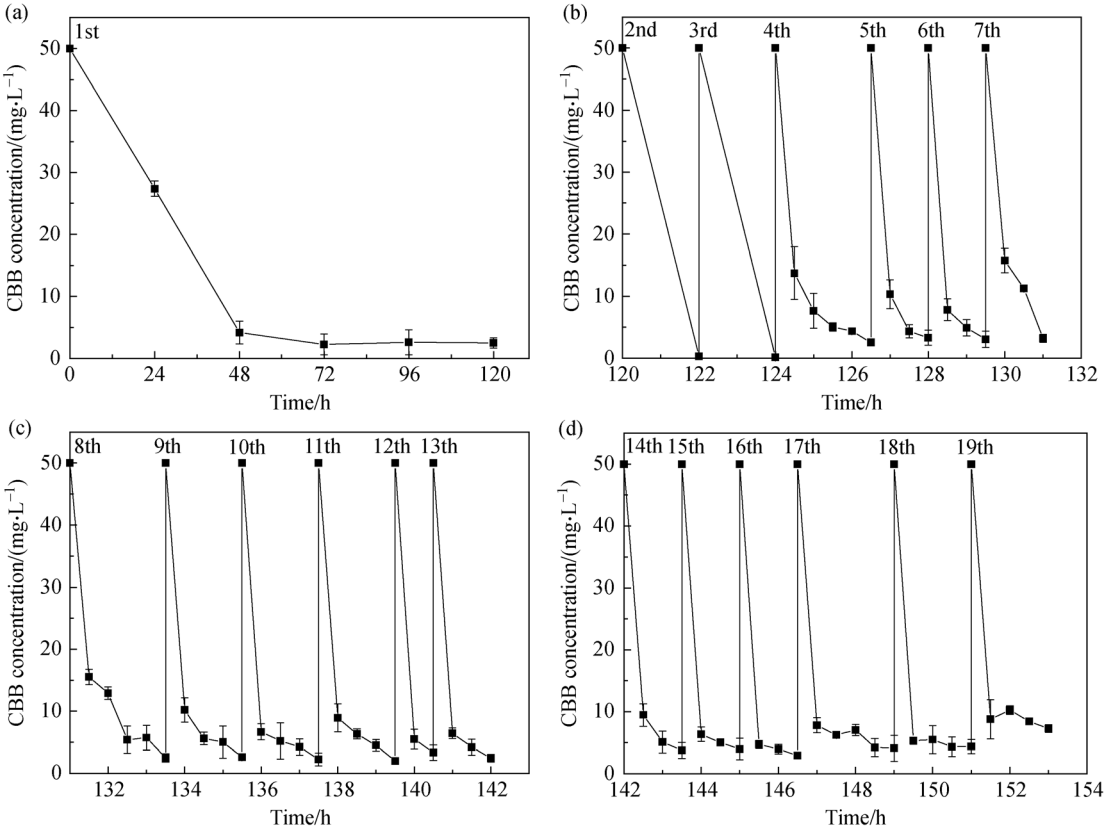

Fig. 4 Decolorization efficiency of the CBB performed with the recycled *L. deliciosus* mycelia through batch processing. (a) First cycle; (b) second to seventh cycle; (c) eighth to thirteenth cycle; (d) fourteenth to nineteenth cycle.

the mycelia needed a certain of time to adapt to the environment thus grew slowly at this stage. With the continuous growth of the mycelia, the dye concentration decreased consecutively until the decolorization rate reached the maximum of 95.51% at 72 h. At this phase, the dye concentration dropped from the initial 50 mg·L^{-1} to about 2 mg·L^{-1}, almost completely removed. After the first dye treatment process, the time used for the continuous batch decolorization was greatly reduced because the mycelia grew integrally in forms of pellets, and it took about 33 h to repeat the second to the nineteenth cycles (Figs. 4(b–d)). At the nineteenth cycle, the dye concentration was kept at 9 mg·L^{-1} within 90 min (50 mg·L^{-1} for each cycle) and the concentration was no longer reduced (Fig. 4(d)), indicating the mycelia pellets reached their maximum utilization for decolorization of the dye. A similar good recycle property is also found in the microorganism of the *Lycinibacillus* sp. RGS, which had an effective decolorization rate of 94% at 21st cycle in removing the dye of Reactive Orange 16 (50 mg·L^{-1} for each cycle) within 220 min [49]. Thus, the *L. deliciosus* mycelia had a prominent recycle property in removing the CBB dye with high efficiency. Most importantly, unlike free mycelia, the pellets formed in this work could be easily separated from the treatment system and reutilized with low costs.

3.4 CBB degradation enzymes analysis

In general, fungi extracellular enzymes play a vital role in dye biodegradation process, such as laccase, MnP and LiP. These enzymes usually have broad-spectrum catalytic degradability and can degrade certain complex refractory substances. As shown in Fig. 5, the variation of lignin oxidase activity, pH value and biomass during decolorization process were investigated. Figure 5(a) shows the maximum enzyme activity of LiP was 121.65 ± 11.2 U·L^{-1}, 36.77 ± 4.8 U·L^{-1} of MnP and 2.85 ± 0.3 U·L^{-1} of laccase respectively. The laccase showed activities at a lowest level within 5 d of incubation period in this study. By contrast, in the white rot fungi (*Lenzites elegans* WDP2)—dye decolorization system the results indicated the laccase enzyme played a major role in decolorization [38]. Some research reported only LiP and MnP enzyme activity was detected during the dye degradation process [18,50]. That is to say, in terms of the dye degradation process laccase, LiP and MnP or a combination of them may function distinctively in different fungi species [43].

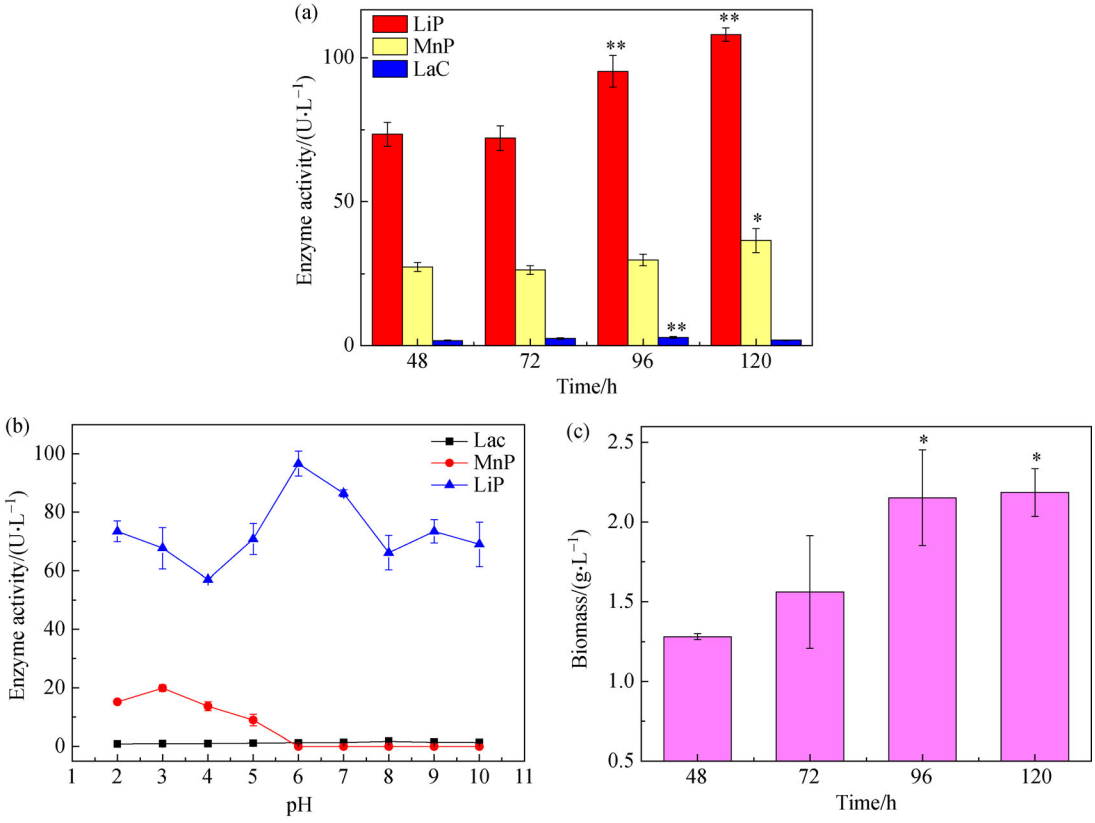

Fig. 5 Variation of extracellular enzymes activity, biomass and pH during the decolorization process with the mycelia. Comparisons were made regarding significant differences of the first point of 48 h at $^{*}P < 0.05$ and $^{**}P < 0.01$, respectively.

In the present study, the LiP and MnP showed a relatively higher enzyme activity, indicating the possible involvement of these two enzymes in triphenylmethane dye decolorization.

At the same time, from Fig. 5(b) it can be seen that the pH value of the treatment broth decreased from the initial value of 5.0 to 4.26, then increased to 4.61 after complete decolorization, while the overall pH variation showed a decreasing trend. Besides, the biomass of LD mycelia increased to 2.18 $g \cdot L^{-1}$ at 120 h (Fig. 5(c)). It indicates that some acidic metabolites were produced during the degradation process. Generally speaking, a weak acidic environment is more beneficial to the degradation of dye compounds [45].

To further investigate the effects of potential environmental factors, the enzymatic properties of the above three lignin enzymes produced by LD were measured under different temperature and pH conditions. It can be seen that the enzyme activity of LiP changed in a typical manner of increasing to the maximum value (81.01 $U \cdot L^{-1}$) at 35 °C before decreasing to 63.30 $U \cdot L^{-1}$ at 40 °C; afterwards it remained relatively stable as temperature further increased (Fig. 6(a)). In comparison, the optimal temperature of MnP was 30 °C, and the enzyme activity decreased dramatically though there was a slightly upward trend after 45 °C (Fig. 6(a)). Nevertheless, the enzyme activity of laccase displayed no significant differences with the temperature rising up to 70 °C (Fig. 6(a)). Figure 6(b) shows the optimum pH of the three enzymes was also distinctive. With the increase of pH values, the overall variation trends of pH were similar to those of the temperature. As can be seen from Fig. 6(b), the optimum pH condition of LiP was 6.0, while the MnP was 3.0. It further manifested that the two enzymes involved in the study were inclined to be activated under acid environment.

In terms of specific enzymes and substrates, V_{max} and K_m are characteristic parameters, which are closely related to the pH and the temperature of the reaction systems. In this study, the enzyme activities of extracellular laccase, MnP and LiP were determined at the optimum temperature and pH conditions with ABTS, $MnSO_4$ and veratryl alcohol as respective substrates. According to the Lineweaver-Burk diagram, the kinetic constants of enzymes to substrates were calculated using the formula below:

$$1/V = 1/V_{max} + (K_m/V_{max}) \times (1/[S]). \quad (4)$$

As shown in Table 1, in light of enzymatic reaction, K_m value is an important indicator of enzyme dynamic

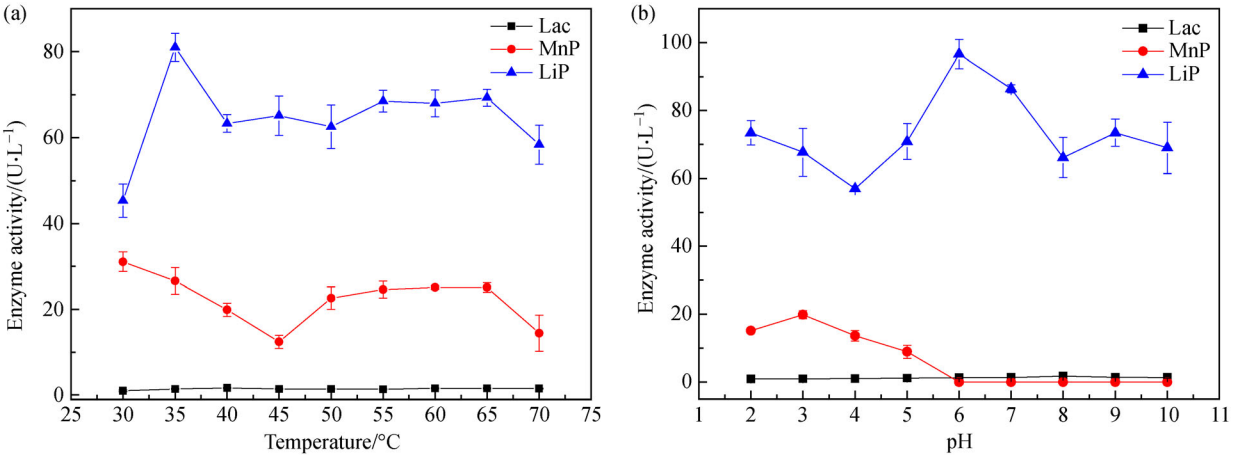

Fig. 6 Effects of temperature and pH on extracellular enzyme activities produced by the mycelia.

property, which reflects the affinity of the enzyme to the substrate. The smaller the K_m value is, the greater affinity of the enzyme to the substrate and the easier the enzymatic reaction. The LiP had the smallest K_m value of 0.633 mmol·L^{-1} and the maximum V_{max} of 30.303 U·L^{-1}, indicating a great deal of LiP enzyme's production during the degradation process. However, although the K_m value of laccase was relatively a bigger one (5.413 mmol·L^{-1}), the maximum V_{max} of laccase was too small (0.09 U·L^{-1}) to lead the role.

3.5 Decolorization and biodegradation analysis

Both SEM and IFM showed that the surface morphology of the fungus was more amorphous after CBB decolorization (Fig. 1S, cf. Electronic Supplementary Material, ESM). Moreover, from the observation of SEM, it can be seen that the mycelia became thicker and more adhesive, which may be attributed to the adsorption of the dye that stimulate the secretion of some viscous substances. From the XRD patterns in Fig. 2S(a) (cf. ESM), it can be seen that the pure CBB had a distinct peak appearing at 19.1°, 28.1°, 32.2°, 33.9°, 38.6° and 48.8°, respectively. Figure 2S(b) was the pattern of *L. deliciosus* mycelia before decolorization, indicating a broad peak at 21.5°; while Figs. 2S(c,d) were the spectra after decolorization treatment for 3 d and 5 d, they also showed corresponding broad peaks at 20.6° and 20.5°, which were similar to the peak location presented in the Fig. 2S(b) before decolorization. In other words, no typical peaks of CBB were found in the treatment samples; CBB dye could be converted during the decolorization treatment, and the bioadsorption and biodegradation may occur simultaneously.

Table 1 The kinetic parameters of extracellular enzymes produced by *L. deliciosus* mycelia

Parameters	LiP	MnP	Laccase
K_m/(mmol·L^{-1})	0.633	1.503	5.413
V_{max}/(U·L^{-1})	30.303	10.881	0.09

To investigate whether conversion occurred during the process, the substances contained in the final treatment solutions were measured by UV-Vis spectrometry in Fig. 3S (cf. ESM). Compared with the CBB standard, the characteristic adsorption peaks at 588 nm disappeared in samples of 25, 50, 100, 200, 400, 600 mg·L^{-1}, indicating that CBB probably transformed to other substance during the process. In comparison, in the sample from LCM concentration of 800 mg·L^{-1}, the adsorption peak presented at 588 nm considerably decreased but not disappeared, indicating that part of the dye still existed in the final treatment solution. This was consistent with the dye removal analysis of the 800 mg·L^{-1} LCM samples, in which the final decolorization rate was only 57.73% after 96 h. The decrease or disappearance of absorption peaks indicated the possible occurrence of biodegradation in which the chromophoric groups may be degraded [51].

The spectrum of the control (Fig. 4S(a), cf. ESM) showed both a broad peak at 3446 cm^{-1} due to the stretching of N–H groups, and peaks at 1575 cm^{-1} and 1500 cm^{-1} due to phenyl rings. In addition, a peak at 2968 cm^{-1} of asymmetric –CH_3 stretch and overtone bond of C–H stretching at 1787 cm^{-1} were observed. The peak at 1388 cm^{-1} represented the primary aromatic amines with C–N bond vibration while the peak at 1170 cm^{-1} was related to C–O bond stretching. The peak at 1028 and 609 cm^{-1} indicated the stretching of sulfonic groups and the peak at 2181 cm^{-1} showed C = C stretching vibration. The extracted metabolites (Fig. 4S(b)) showed the peak at 3446 cm^{-1} indicating the N–H bond still existed. The peak at 1159 cm^{-1} may be ascribed to the stretching of C – O bond. As compared to the control, the disappearance of peak at 1575 and 1500 cm^{-1} indicated the possible breakage of

phenyl rings, resulting from degradation of CBB by the mycelia. Meanwhile, the disappearance of peak at 1028 and 609 cm^{-1} also proved the removal of sulfonic groups of CBB. These results could confirm a preliminary assumption, namely, the bioadsorption and biodegradation did occur during the process in this work. Therefore, the *L. deliciosus* mycelia pellets could transform the triphenylmethane dyes like CBB to a great extent.

By far, few reports have addressed the degradation of CBB dye with fungi. Here, we proposed a degradation pathway of CBB dye based on the results, as shown in Fig. 7. During the process, the (a) CBB dye was first converted to (b) tetraethyl Michler's ketone and (c) phenol derivative by the mycelia of *L. deliciosus*, and then transformed to (d) *p*-formaldehyde phenylacetic acid and (e) hydroquinone. These substrates may be further converted to simple open chain hydrocarbons. The hypothesis of forming benzene free ring and simple compound was also confirmed by FTIR results. Researchers reported the conversion procedure of triphenylmethane dyes by microorganisms, for instance, the degradation process of crystal violet to phenol [8] and the transformation of malachite green to Michlers ketone or DLBP by *Micrococcus* sp. strain BD15 [4].

3.6 Thermal stability analysis

Before decolorization, the TG curve (Fig. 5S(a), cf. ESM) showed the fungal mycelia decomposed evidently after 200 °C and the drastic decomposition occurred near 292 °C. Consequently, after the mycelia adsorbed the dye, the TG curve (Fig. 5S(b)) showed the mycelia experienced a drastic decomposition phase and began to lose weight after 240 °C. The first derivative (DTG) curve showed a peak at 279 °C, indicating the drastic decomposition happened at this point, probably due to the decomposition of the mycelia and subsequent dye release from the system. In the meantime, the temperature dropped at the drastic decomposition stage, namely from 292 °C to 279 °C, indicating a weak growth status of the mycelia after decolorization. These results were consistent with the above SEM observation (Fig. 1S, cf. ESM), in which the fungus became more amorphous. Most of the weightlessness was due to the pyrolysis of the fungus, and the

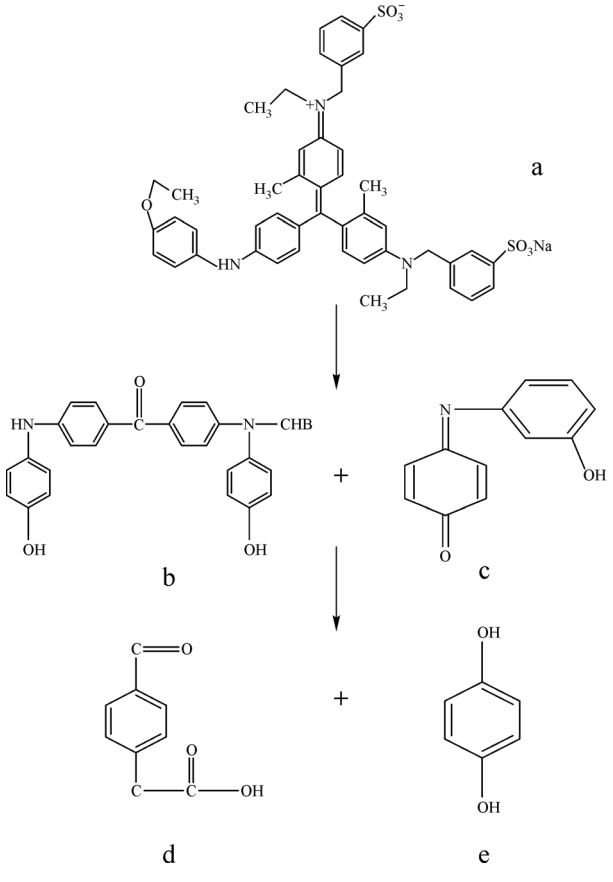

Fig. 7 The supposed degradation pathway of CBB by the mycelia of *L. deliciosus*.

moisture and volatiles missed at about 150 °C, which was similar to Agrawal's result [41].

3.7 Phytotoxicity and microbial toxicity assessments

Some synthetic dyes like triphenylmethane dyes, azo dyes are reported to be highly toxic to organisms and their degradation intermediates are even more poisonous than that of the parent compound [27,43]. Therefore, the toxicity of the CBB dye and its degraded products were evaluated.

As shown in Fig. 8, the CBB dye solution had a significant toxic effect on wheat seeds' germination, plumule and root growth compared with the distilled water treated group. With the increase of treatment time, the influence/toxicity of the obtained decolorized water on wheat seeds growth displayed a decreasing trend visibly. The germination rate, plumule and root length were increasing gradually up to the maximum value of 82.22%, 2.95 ± 0.43 and 2.66 ± 0.58 cm with decolorized water after 120 h treatment, respectively. It confirmed that the toxicity of CBB was substantially reduced after degradation and decolorization processes. According to Shabbir's report, the germination index (GI) value below 50% suggests a high phytotoxicity, while a 50%–80% GI value indicates a moderate phytotoxicity with 80% and above suggesting non-toxicity [8]. Thus, the obtained decolorized water in this work was non-toxic.

Similar results were found in the *E. coli* contact inhibition experiments (Table 2). It shows that the pure CBB dye solution had the highest toxicity; the inhibition rate was 44.8% initially, however, after 48, 72, 96 and 120 h treatment, the inhibition rates of *E. coli* decreased sharply, and no inhibition effect was observed after 120 h of treatment, indicating the toxicity of the dye water was gradually reduced and became non-toxic finally.

Besides, the CBB dye solution had a profound effect on the body length and movement behavior of *C. elegans*. In

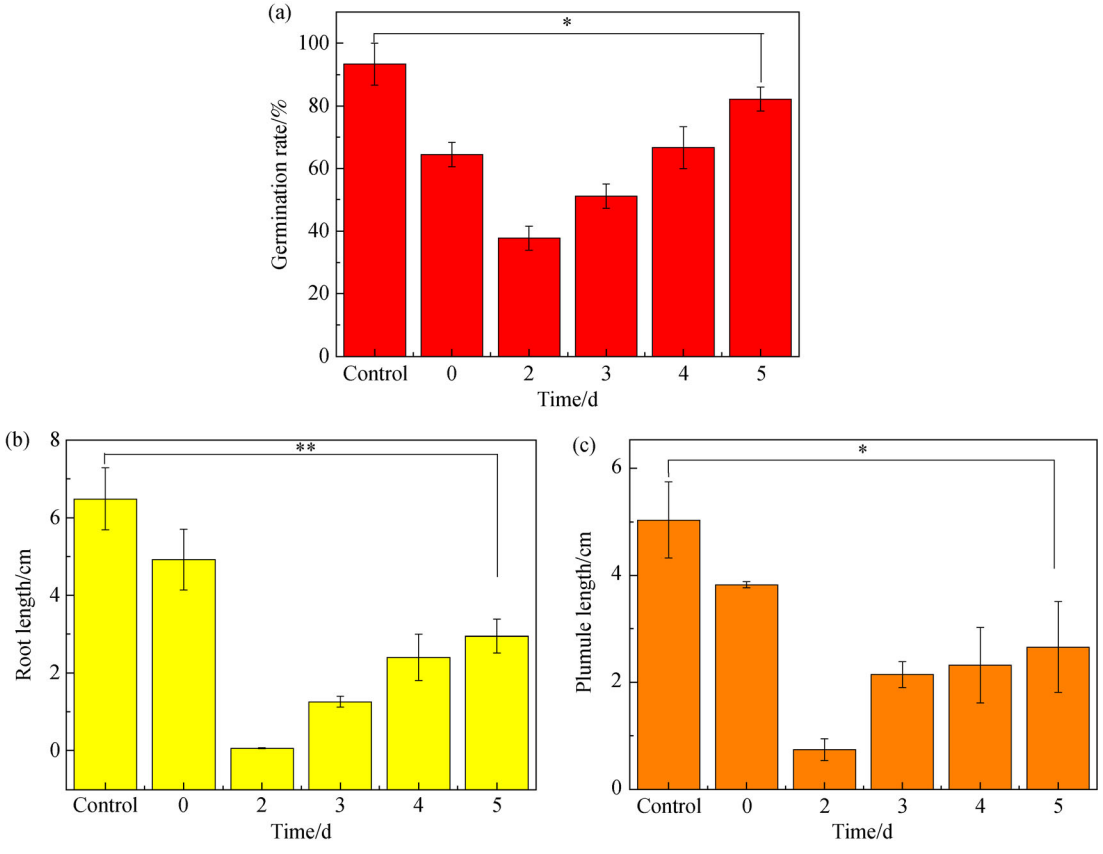

Fig. 8 Phytotoxicity of the decolorized water on wheat seeds growth. (a) Germination rate; (b) root length; (c) plumule length. * indicates statistical significance at $P < 0.05$; ** indicates statistical significance at $P < 0.01$.

Table 2 Toxicity of the CBB dye solution (0 h) and the decolorized water on growth of *E. coli* in plate

Time/h	0	48	72	96	120
Inhibition rate/%	44.08 ± 2.1	41.32 ± 2.3	16.53 ± 0.6	1.10 ± 0.2	0

comparison, the obtained decolorized water (96, 120 h) barely affected the body length (Fig. 9(a)) and movement behaviors (Figs. 9(b) and 9(c)), indicating the decolorized water was non-toxic. Meanwhile, according to the results of spontaneous fluorescence intensity of *C. elegans* (Fig. 10), the decolorized water (after 48 h treatment) had no significant effect on the accumulation of lipofuscin in *C. elegans*, one of the important characteristics of cell damage. The acute exposure of hexabromocyclododecane with a concentration greater than 20 nmol·L^{-1} significantly reduced the body bending of nematodes [52]. Herein the results confirmed that the decolorized water was non-toxic and had no oxidative stress on *C. elegans*.

4 Conclusions

In the current work, the mycelia of a wild edible fungus of *L. deliciosus* used for effective removal of CBB dye were evaluated, which provided a viewpoint of biological method for treating dye wastewater. The mycelia could realize decolorization rate of 99.19% with 600 mg·L^{-1} CBB samples within 96 h, at a maximal removal rate of 16.31 mg·L^{-1}·h. The continuous batch treatment of the dye by the mycelia pellets demonstrated good recyclability. The fungal strain proved to be an excellent candidate for the removal of triphenylmethane dye like CBB within a broad range of temperature and agitation speed, providing a basis for practical design of treatment protocol. Furthermore, the fungus showed an efficient degradation of CBB dye with mainly two kinds of extracellular enzymes involved, namely LiP and MnP. The kinetic parameters of enzymes also proved LiP had good affinity with substrates. UV-visible spectra and FTIR studies suggested that the dye removal was attributed to the synergy effects of adsorption and degradation of the mycelia. Compared with the results of previous researches on microbiological treatment, the fungi cultivated in this study were more efficient in the presence of high concentrations of CBB. The toxicity of the decolorized water on wheat seed germination, *E. coli* and *C. elegans* decreased dramatically compared with pure CBB dye solution, indicating the occurrence of dye degradation process. Thus, the fungi mycelia could be potentially used for environment-friendly treatment of CBB dye wastewater.

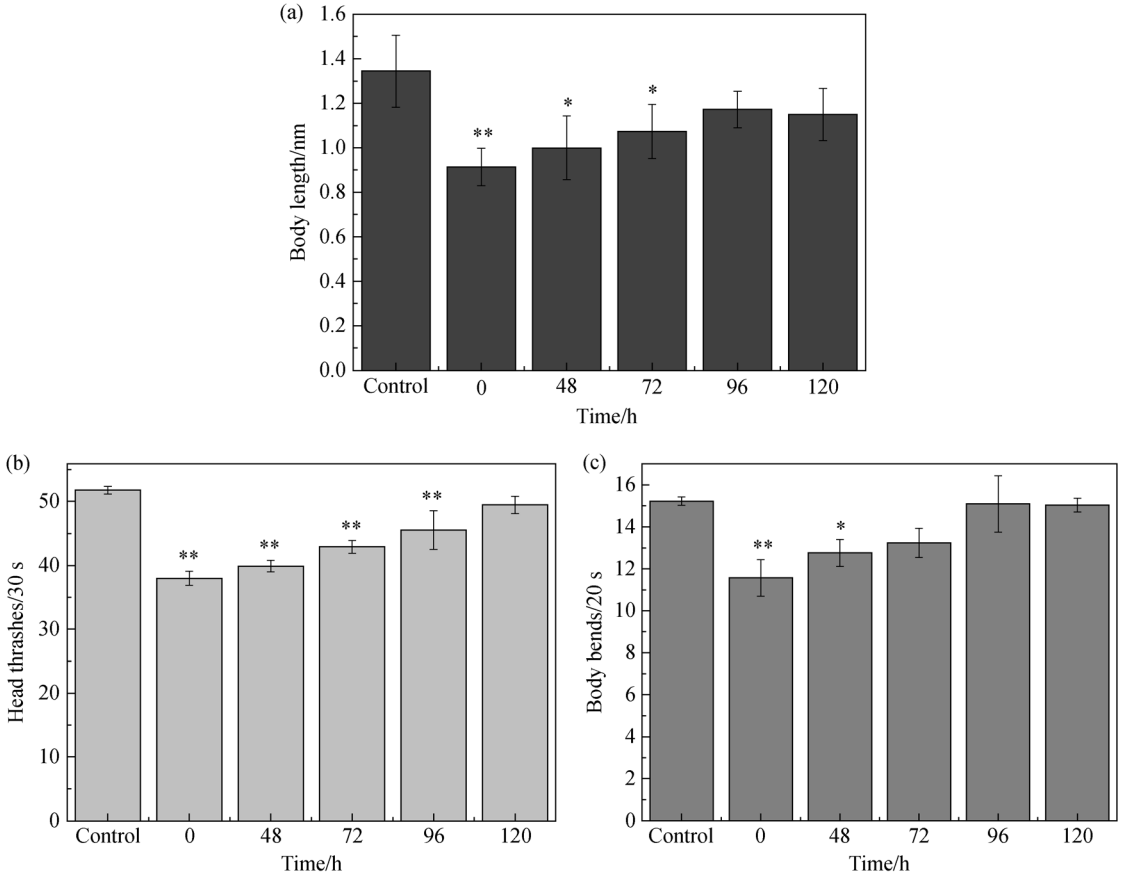

Fig. 9 Effects of the decolorized water on body length and locomotion behavior of *C. elegans*. (a) Body length; (b) head thrashes; (c) body bends. * indicates statistical significance at $P < 0.05$; ** indicates statistical significance at $P < 0.01$.

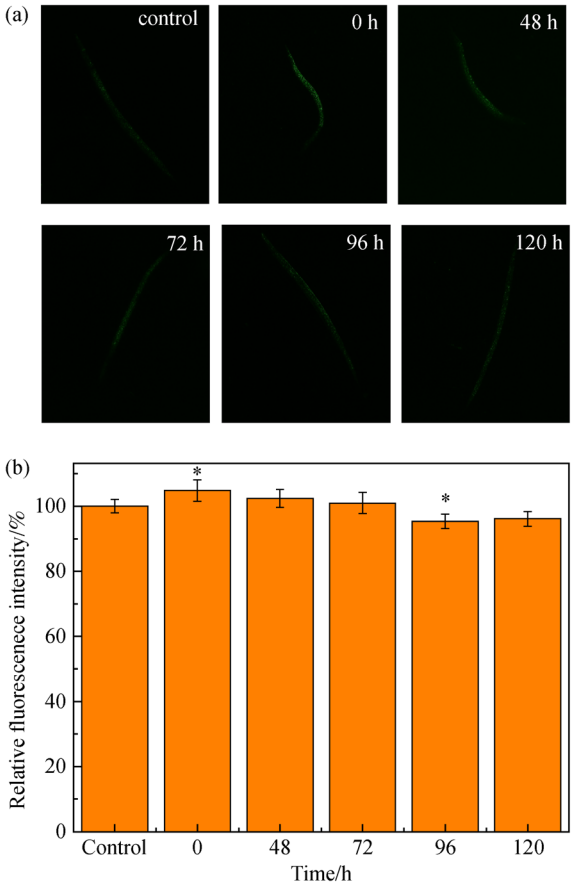

Fig. 10 Effects of the decolorized water on *C. elegans*. (a) Representative images showing the intestinal autofluorescence in *C. elegans* after exposure to the decolorized water at different treatment periods; (b) comparison of intestinal autofluorescence intensities in *C. elegans* after exposure to the decolorized water at different treatment periods. * indicates statistical significance at $P < 0.05$; ** indicates statistical significance at $P < 0.01$.

Acknowledgements This work was supported by the Anhui Provincial Program on Key Research and Development Project (Grant No. 202004a06020021), the National Natural Science Foundation of China (Grant No. 21606002), the Natural Science Foundation of Anhui Province (CN) (Grant No. 1708085QC64) and the Undergraduate Research Training Programs for Innovation (Grant Nos. 201910357069, S201910357427).

Electronic Supplementary Material Supplementary material is available in the online version of this article at https://doi.org/10.1007/s11705-020-1952-7 and is accessible for authorized users.

References

1. Mostafa A A, Elshikh M S, Al-Askar A A, Hadibarata T, Yuniarto A, Syafiuddin A. Decolorization and biotransformation pathway of textile dye by *Cylindrocephalum aurelium.* Bioprocess and Biosystems Engineering, 2019, 42(9): 1483–1494
2. Chakraborty S, Basak B, Dutta S, Bhunia B, Dey A. Decolorization and biodegradation of Congo red dye by a novel white rot fungus *Alternaria alternata* CMERI F6. Bioresource Technology, 2013, 147: 662–666
3. Hu M R, Chao Y P, Zhang G Q, Xue Z Q, Qian S. Laccase-mediator system in the decolorization of different types of recalcitrant dyes. Journal of Industrial Microbiology & Biotechnology, 2009, 36(1): 45–51
4. Yang X, Zheng J, Lu Y, Jia R. Degradation and detoxification of the triphenylmethane dye malachite green catalyzed by crude manganese peroxidase from *Irpex lacteus* F17. Environmental Science and Pollution Research International, 2016, 23(10): 9585–9597
5. Chengalroyen M D, Dabbs E R. The microbial degradation of azo dyes: mini review. World Journal of Microbiology & Biotechnology, 2013, 29(3): 389–399
6. Saratale R G, Saratale G D, Chang J S, Govindwar S P. Bacterial decolorization and degradation of azo dyes: a review. Journal of the Taiwan Institute of Chemical Engineers, 2011, 42(1): 138–157
7. Wang N, Chu Y, Wu F, Zhao Z, Xu X. Decolorization and degradation of Congo red by a newly isolated white rot fungus, *Ceriporia lacerata*, from decayed mulberry branches. International Biodeterioration & Biodegradation, 2017, 117: 236–244
8. Shabbir S, Faheem M, Wu Y. Decolorization of high concentration crystal violet by periphyton bioreactors and potential of effluent reuse for agricultural purposes. Journal of Cleaner Production, 2018, 170: 425–436
9. Boonyakamol A, Imai T, Chairattanamanokorn P, Higuchi T, Sekine M. Key factors regarding decolorization of synthetic anthraquinone and azo dyes. Applied Biochemistry and Biotechnology, 2009, 158(1): 180–191
10. Mueangtoom K, Kittl R, Mann O, Haltrich D, Ludwig R. Low pH dye decolorization with ascomycete *Lamprospora wrightii laccase.* Biotechnology Journal, 2010, 5(8): 857–870
11. Przystaś W, Zabłocka-Godlewska E, Grabińska-Sota E. Biological removal of azo and triphenylmethane dyes and toxicity of process by-products. Water, Air, and Soil Pollution, 2012, 223(4): 1581–1592
12. Yang X, Wang J, Zhao X, Wang Q, Xue R. Increasing manganese peroxidase production and biodecolorization of triphenylmethane dyes by novel fungal consortium. Bioresource Technology, 2011, 102(22): 10535–10541
13. Kumar K V, Sivanesan S, Ramamurthi V. Adsorption of malachite green onto *Pithophora* sp., a fresh water algae: equilibrium and kinetic modelling. Process Biochemistry, 2005, 40(8): 2865–2872
14. He H, Yang S, Yu K, Ju Y, Sun C, Wang L. Microwave induced catalytic degradation of crystal violet in nano-nickel dioxide suspensions. Journal of Hazardous Materials, 2010, 173(1-3): 393–400
15. Ayed L, Mahdhi A, Cheref A, Bakhrouf A. Decolorization and degradation of azo dye methyl red by an isolated *Sphingomonas paucimobilis*: biotoxicity and metabolites characterization. Desalination, 2011, 274(1-3): 272–277
16. Verma P, Madamwar D. Decolourization of synthetic dyes by a newly isolated strain of *Serratia marcescens.* World Journal of Microbiology & Biotechnology, 2003, 19(6): 615–618
17. Ozdemir S, Cirik K, Akman D, Sahinkaya E, Cinar O. Treatment of azo dye-containing synthetic textile dye effluent using sulfidogenic anaerobic baffled reactor. Bioresource Technology, 2013, 146: 135–

143

18. He X, Song C, Li Y, Wang N, Xu L, Han X, Wei D. Efficient degradation of azo dyes by a newly isolated fungus *Trichoderma tomentosum* under non-sterile conditions. Ecotoxicology and Environmental Safety, 2018, 150: 232–239
19. Vajnhandl S, Le Marechal A M. Ultrasound in textile dyeing and the decolouration/mineralization of textile dyes. Dyes and Pigments, 2005, 65(2): 89–101
20. Veisi H, Razeghi S, Mohammadi P, Hemmati S. Silver nanoparticles decorated on thiol-modified magnetite nanoparticles (Fe_3O_4/SiO_2-Pr-S-Ag) as a recyclable nanocatalyst for degradation of organic dyes. Materials Science & Engineering C—Materials for Biological Applications, 2019, 97: 624–631
21. Bankole P O, Adekunle A A, Govindwar S P. Biodegradation of a monochlorotriazine dye, cibacron brilliant red 3B-A in solid state fermentation by wood-rot fungal consortium, *Daldinia concentrica* and *Xylaria polymorpha* co-biomass decolorization of cibacron brilliant red 3B-A dye. International Journal of Biological Macromolecules, 2018, 120(A): 19–27
22. Salami F, Habibi Z, Yousefi M, Mohammadi M. Covalent immobilization of laccase by one pot three component reaction and its application in the decolorization of textile dyes. International Journal of Biological Macromolecules, 2018, 120(A): 144–151
23. Muthukumaran C, Sivakumar V M, Thirumarimurugan M. Adsorption isotherms and kinetic studies of crystal violet dye removal from aqueous solution using surfactant modified magnetic nanoadsorbent. Journal of the Taiwan Institute of Chemical Engineers, 2016, 63: 354–362
24. Watharkar A D, Khandare R V, Kamble A A, Mulla A Y, Govindwar S P, Jadhav J P. Phytoremediation potential of *Petunia grandiflora* Juss., an ornamental plant to degrade a disperse, disulfonated triphenylmethane textile dye brilliant blue G. Environmental Science and Pollution Research International, 2013, 20(2): 939–949
25. Salleh M A M, Mahmoud D K, Karim W A W A, Idris A. Cationic and anionic dye adsorption by agricultural solid wastes: a comprehensive review. Desalination, 2011, 280(1-3): 1–13
26. Gupta V K, Khamparia S, Tyagi I, Jaspal D, Malviya A. Decolorization of mixture of dyes: a critical review. Global Journal of Environmental Science and Management, 2015, 1(1): 71–94
27. Bharagava R N, Mani S, Mulla S I, Saratale G D. Degradation and decolourization potential of an ligninolytic enzyme producing *Aeromonas hydrophila* for crystal violet dye and its phytotoxicity evaluation. Ecotoxicology and Environmental Safety, 2018, 156: 166–175
28. van der Zee F P, Villaverde S. Combined anaerobic–aerobic treatment of azo dyes—a short review of bioreactor studies. Water Research, 2005, 39(8): 1425–1440
29. Anastasi A, Spina F, Romagnolo A, Tigini V, Prigione V, Varese G C. Integrated fungal biomass and activated sludge treatment for textile wastewaters bioremediation. Bioresource Technology, 2012, 123: 106–111
30. Zerva A, Zervakis G I, Christakopoulos P, Topakas E. Degradation of olive mill wastewater by the induced extracellular ligninolytic enzymes of two wood-rot fungi. Journal of Environmental Management, 2017, 203: 791–798
31. Rajesh R, Iyer S S, Ezhilan J, Kumar S S, Venkatesan R. Graphene oxide supported copper oxide nanoneedles: an efficient hybrid material for removal of toxic azo dyes. Spectrochimica Acta. Part A: Molecular and Biomolecular Spectroscopy, 2016, 166: 49–55
32. Saratale R G, Gandhi S S, Purankar M V, Kurade M B, Govindwar S P, Oh S E, Saratale G D. Decolorization and detoxification of sulfonated azo dye C.I. Remazol Red and textile effluent by isolated *Lysinibacillus* sp. RGS. Journal of Bioscience and Bioengineering, 2013, 115(6): 658–667
33. Ramsay J A, Mok W H W, Luu Y S, Savage M. Decoloration of textile dyes by alginate-immobilized *Trametes versicolor*. Chemosphere, 2005, 61(7): 956–964
34. Munck C, Thierry E, Gräßle S, Chen S H, Ting A S Y. Biofilm formation of filamentous fungi *Coriolopsis* sp. on simple muslin cloth to enhance removal of triphenylmethane dyes. Journal of Environmental Management, 2018, 214: 261–266
35. Paz A, Carballo J, Pérez M J, Domínguez J M. Biological treatment of model dyes and textile wastewaters. Chemosphere, 2017, 181: 168–177
36. Janović B S, Mićić Vićovac M L, Vujčić Z M, Vujčić M T. Tailor-made biocatalysts based on scarcely studied acidic horseradish peroxidase for biodegradation of reactive dyes. Environmental Science and Pollution Research International, 2017, 24(4): 3923–3933
37. Kulkarni A N, Watharkar A D, Rane N R, Jeon B, Govindwar S P. Decolorization and detoxification of dye mixture and textile effluent by lichen *Dermatocarpon vellereceum* in fixed bed upflow bioreactor with subsequent oxidative stress study. Ecotoxicology and Environmental Safety, 2018, 148: 17–25
38. Pandey R K, Tewari S, Tewari L. Lignolytic mushroom *Lenzites elegans* WDP2: laccase production, characterization, and bioremediation of synthetic dyes. Ecotoxicology and Environmental Safety, 2018, 158: 50–58
39. Zhao W, Wei Z, Zhang L, Wu X, Wang X. Cr doped SnS_2 nanoflowers: preparation, characterization and photocatalytic decolorization. Materials Science in Semiconductor Processing, 2018, 88: 173–180
40. Shabbir S, Faheem M, Ali N, Kerr P G, Wu Y. Periphyton biofilms: a novel and natural biological system for the effective removal of sulphonated azo dye methyl orange by synergistic mechanism. Chemosphere, 2017, 167: 236–246
41. Agrawal A, Chakraborty S. A kinetic study of pyrolysis and combustion of microalgae *Chlorella vulgaris* using thermo-gravimetric analysis. Bioresource Technology, 2013, 128: 72–80
42. Legerska B, Chmelova D, Ondrejovic M. Decolourization and detoxification of monoazo dyes by laccase from the white-rot fungus Trametes versicolor. Journal of Biotechnology, 2018, 285: 84–90
43. Kumar R, Negi S, Sharma P, Prasher I B, Chaudhary S, Dhau J S, Umar A. Wastewater cleanup using *Phlebia acerina* fungi: an insight into mycoremediation. Journal of Environmental Management, 2018, 228: 130–139
44. Wang M, Zhang Q, Yao S. A novel biosorbent formed of marine-derived *Penicillium janthinellum* mycelial pellets for removing dyes from dye-containing wastewater. Chemical Engineering Journal, 2015, 259: 837–844
45. Daâssi D, Mechichi T, Nasri M, Rodriguez-Couto S. Decolorization

of the metal textile dye Lanaset Grey G by immobilized white-rot fungi. Journal of Environmental Management, 2013, 129: 324–332

46. Vitor V, Corso C R. Decolorization of textile dye by *Candida albicans* isolated from industrial effluents. Journal of Industrial Microbiology & Biotechnology, 2008, 35(11): 1353–1357
47. Shabbir S, Faheem M, Ali N, Kerr P G, Wu Y. Evaluating role of immobilized periphyton in bioremediation of azo dye amaranth. Bioresource Technology, 2017, 225: 395–401
48. Dos Santos A B, Bisschops I A E, Cervantes F J, van Lier J B. Effect of different redox mediators during thermophilic azo dye reduction by anaerobic granular sludge and comparative study between mesophilic (30 °C) and thermophilic (55 °C) treatments for decolourisation of textile wastewaters. Chemosphere, 2004, 55(9): 1149–1157
49. Bedekar P A, Saratale R G, Saratale G D, Govindwar S P. Oxidative stress response in dye degrading bacterium *Lysinibacillus* sp. RGS exposed to reactive orange 16, degradation of RO16 and evaluation of toxicity. Environmental Science and Pollution Research International, 2014, 21(18): 11075–11085
50. Xu J Z, Zhang J L, Hu K H, Zhang W G. The relationship between lignin peroxidase and manganese peroxidase production capacities and cultivation periods of mushrooms. Microbial Biotechnology, 2013, 6(3SI): 241–247
51. Chen S H, Yien Ting A S. Biosorption and biodegradation potential of triphenylmethane dyes by newly discovered *Penicillium simplicissimum* isolated from indoor wastewater sample. International Biodeterioration & Biodegradation, 2015, 103: 1–7
52. Chen H, Guo S, Li H, Zhou D, Cao X, Wang C, Liu Y, Xiang M, Li L, Yu Y. Multi-generational effects and variations of stress response by hexabromocyclododecane (HBCD) exposure in the nematode *Caenorhabditis elegans.* Journal of Environmental Management, 2019, 245: 216–222